

# Bridging Abstraction-Based Hierarchical Control and Moment Matching: A Conceptual Unification

Zirui Niu, Mohammad Fahim Shakib, and Giordano Scariotti

**Abstract**—In this paper, we establish a relation between approximate-simulation-based hierarchical control (ASHC) and moment matching techniques, and build a conceptual bridge between these two frameworks. To this end, we study the two key requirements of the ASHC technique, namely the bounded output discrepancy and the  $M$ -relation, through the lens of moment matching. We show that, in the linear time-invariant case, both requirements can be interpreted in the moment matching perspective through certain system interconnection structures. Building this conceptual bridge provides a foundation for cross-pollination of ideas between these two frameworks.

## I. INTRODUCTION

In the field of computational science and engineering, real-world complex dynamical systems typically require large-scale mathematical models for accurate representations. However, the high dimensionality of those models can result in excessive computational costs for analysis and (control) design, leading to substantial processing time and energy consumption for, *e.g.*, simulations and hardware implementations.

Two prominent methodologies that address these challenges are model order reduction (MOR) and approximate-simulation-based hierarchical control (ASHC). MOR focuses on simplifying high-dimensional models while retaining essential system dynamics, see, *e.g.*, [1]–[3] and references therein for details of different MOR approaches. Instead, ASHC focuses on efficient control design for large-scale systems by decomposing control tasks into hierarchical levels. These levels comprise a simpler model, called abstract system, and an interface function that translates the input from the abstract system back to the original, large-scale system, as depicted in Fig. 1. In such manner, the control synthesis of the large-scale system can be achieved with lower complexity [4]. This ASHC approach has been applied, for instance, to control networked systems [5] and robot systems [4].

In this paper, we establish a relation between the ASHC technique introduced in [4] and the moment-matching-based MOR technique introduced in [6]. We observe that both methods hinge upon the use of specific interconnection structures. On the one hand, moment matching uses system interconnections, shown in Fig. 2, to characterise some key properties, *i.e.*, the so-called moments, to be preserved by the simpler, reduced-order model. This is achieved by studying the interconnection of the large-scale system with a signal generator (Fig. 2(a)) or a filter (Fig. 2(b)) that incorporate

Zirui Niu, Mohammad Fahim Shakib, and Giordano Scariotti are with the Department of Electrical and Electronic Engineering, Imperial College London, SW7 2AZ, London, U.K. [\[zirui.niu20,m.shakib,g.scariotti\]@imperial.ac.uk](mailto:[zirui.niu20,m.shakib,g.scariotti]@imperial.ac.uk).

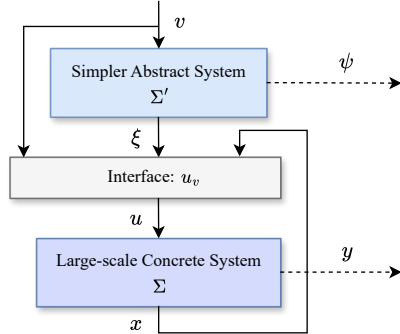


Fig. 1. Hierarchical control system architecture.

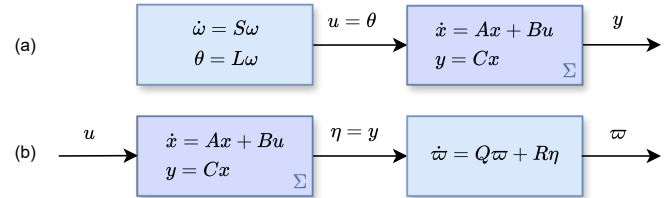


Fig. 2. Illustration of the direct interconnection (a) and the swapped interconnection (b) in moment matching.

the information of the desired behaviours of interest [6]. On the other hand, the hierarchical levels in the ASHC technique hinge on the interconnection structure in Fig. 1, as already described. In studying these interconnections, both techniques rely on the solution of closely related Sylvester equations. This observation hints at a relation between these two methods.

To study this relation, we start with revisiting the fundamentals of moment matching and ASHC techniques. Then we reinterpret the ASHC technique through the lens of moment matching, showing that the two key design requirements proposed in the ASHC technique, namely the bounded output discrepancy and the so-called  $M$ -relation<sup>1</sup>, can be interpreted as moment matching requirements. Based on this result, we provide guidance for future works that aim, on the one hand, at extending various moment matching results, such as nonlinear and data-driven methods, to address ASHC problems, and, on the other hand, at establishing new techniques for control via reduced-order models. In summary, the main contribution of this paper lies in the establishment of a conceptual bridge between the two techniques, showing the possibility that the developed methods in each field can mutually benefit

<sup>1</sup>This is usually called  $\Pi$ -relation in the literature [7]. We changed the letter for notational reasons.

one another. Further works that explore these directions are already in preparation.

The remainder of this paper is organised as follows. Section II provides a brief review of the two techniques. Section III gives the relation between ASHC and moment matching. An illustrative example is presented in Section IV, followed by some concluding remarks in Section V.

**Notation.** The symbols  $\mathbb{C}_0$  and  $\mathbb{C}_{<0}$  denote the set of complex numbers with zero real part and strictly negative real part, respectively, while  $\mathbb{R}_{\geq 0}$  represents the set of non-negative real numbers. The symbol  $I_n$  indicates an  $n \times n$  identity matrix,  $\sigma(A)$  represents the spectrum of the matrix  $A \in \mathbb{R}^{n \times n}$ , while for  $B \in \mathbb{R}^{n \times m}$ ,  $B^\top$  denotes its transpose. A square matrix  $A$  is positive definite if it is symmetric and all its eigenvalues are positive. Given a bounded function  $x : \mathbb{R} \rightarrow \mathbb{R}^n$ ,  $\|x\|_\infty$  denotes its  $L^\infty$  norm defined by  $L^\infty := \sup_{t \geq 0} \|x(t)\|$ , where  $\|\cdot\|$  indicates the Euclidean norm. A function  $\gamma : \mathbb{R}_{\geq 0} \rightarrow \mathbb{R}_{\geq 0}$  belongs to class  $\mathcal{K}$  if it is continuous, strictly increasing, and satisfies  $\gamma(0) = 0$ .

## II. REVIEW OF MOMENT MATCHING AND ASHC TECHNIQUES

In this section, we recall the moment matching and ASHC techniques for a class of (large-scale) linear time-invariant (LTI) systems of the form

$$\Sigma : \quad \dot{x} = Ax + Bu, \quad y = Cx, \quad (1)$$

where  $x(t) \in \mathbb{R}^n$ ,  $u(t) \in \mathbb{R}^m$ , and  $y(t) \in \mathbb{R}^p$ . The real-valued matrices  $A$ ,  $B$ , and  $C$  are of appropriate dimensions and, without loss of generality, assumed to satisfy  $\text{rank}(B) = m$  and  $\text{rank}(C) = p$ . Then, both the moment matching and ASHC techniques aim to find a simpler LTI model in the form

$$\Sigma' : \quad \dot{\xi} = F\xi + Gv, \quad \psi = H\xi, \quad (2)$$

where  $\xi(t) \in \mathbb{R}^{\hat{n}}$ ,  $v(t) \in \mathbb{R}^{\hat{m}}$ , and  $\psi(t) \in \mathbb{R}^p$ , and the real-valued matrices  $F$ ,  $G$ , and  $H$  are of appropriate dimensions, with order  $\hat{n} \leq n$ . Note that in the MOR technique, systems (1) and (2) are called the *full-* and the *reduced-order model*, respectively, with the same number of inputs, *i.e.*,  $\hat{m} = m$ . In the ASHC technique, instead, the simpler system (2) is called the *abstract system* or *abstraction*, while the large-scale system (1) is called the *concrete system*. The number of inputs of these two systems is not necessarily the same.

### A. Moment Matching

We first revisit the moment matching method, starting with the definition of moment of system (1).

**Definition 1** ([3]): Consider system (1) and matrices  $S \in \mathbb{R}^{\hat{n} \times \hat{n}}$  and  $Q \in \mathbb{R}^{\hat{n} \times \hat{n}}$  with their spectra satisfying  $\sigma(S) \cap \sigma(A) = \emptyset$  and  $\sigma(Q) \cap \sigma(A) = \emptyset$ . Let  $L \in \mathbb{R}^{m \times \hat{n}}$  and  $R \in \mathbb{R}^{\hat{n} \times p}$  be any two matrices such that the pair  $(S, L)$  is observable and the pair  $(Q, R)$  is reachable. Then the matrices  $C\Pi$  and  $\Upsilon B$  are called the *moments* of system (1) at  $(S, L)$  and  $(Q, R)$  respectively, where  $\Pi \in \mathbb{R}^{n \times \hat{n}}$  is the unique solution of the Sylvester equation

$$\Pi S = A\Pi + BL, \quad (3)$$

and  $\Upsilon \in \mathbb{R}^{\hat{n} \times n}$  is the unique solution of the Sylvester equation

$$Q\Pi = \Upsilon A + RC. \quad (4) \blacksquare$$

**Remark 1:** Originally moments were defined in the Laplace domain [1]. More precisely, the  $k$ -th moment of a single-input single-output system (1) at an interpolation point  $s \in \mathbb{C} \setminus \sigma(A)$  is defined as the  $k$ -th coefficient of the Laurent series expansion of the transfer function of system (1) at  $s$ . The moments computed at interpolation points equal to the eigenvalues of  $S$  and  $Q$  are nothing else than the elements of the matrices  $C\Pi$  and  $\Upsilon B$ , see [6], [8], and [9] for the multiple-input, multiple-output case.

It is possible to show [6] that the model

$$\dot{\xi} = (S - GL)\xi + Gu, \quad \psi = C\Pi\xi \quad (5)$$

matches the moments of (1) (meaning that the moments of the two models are identical) at  $(S, L)$  for any  $G$  such that  $\sigma(S) \cap \sigma(S - GL) = \emptyset$ . Likewise, the model

$$\dot{\xi} = (Q - RH)\xi + \Upsilon Bu, \quad \psi = H\xi \quad (6)$$

matches the moments of (1) at  $(Q, R)$  for any  $H$  such that  $\sigma(Q - RH) \cap \sigma(Q) = \emptyset$ . Moreover, a model that matches the moments of (1) at  $(S, L)$  and  $(Q, R)$  simultaneously is called two-sided moment matching model. This two-sided matching can be achieved, for example, by model (5) with  $G = (\Upsilon\Pi)^{-1}\Upsilon B$ , or by model (6) with  $H = C\Pi(\Upsilon\Pi)^{-1}$ , provided that  $\Upsilon\Pi$  is invertible, see [3] for more details.

Inspired by the regulator theory [10], the Sylvester equations (3) and (4) also induce a connection between moments and the steady-state output responses of two interconnection structures, namely the direct and swapped interconnections, as depicted in Fig. 2 and summarized as follows.

**Theorem 1** ([3]): Consider system (1) and suppose  $\sigma(A) \subset \mathbb{C}_{<0}$ . Let  $S \in \mathbb{R}^{\hat{n} \times \hat{n}}$  and  $Q \in \mathbb{R}^{\hat{n} \times \hat{n}}$  be any two matrices with simple eigenvalues satisfying  $\sigma(S) \subset \mathbb{C}_0$  and  $\sigma(Q) \subset \mathbb{C}_0$  with  $\sigma(S) \cap \sigma(Q) = \emptyset$ . Let  $L \in \mathbb{R}^{m \times \hat{n}}$  and  $R \in \mathbb{R}^{\hat{n} \times p}$  be any two matrices such that the pair  $(S, L)$  is observable and the pair  $(Q, R)$  is reachable. Then the following statements hold.

- The moment at  $(S, L)$  admits a one-to-one relation with the steady-state of output  $y$  of the (direct) interconnection between system (1) and the signal generator

$$\dot{\omega} = Sw, \quad \theta = L\omega, \quad (7)$$

via  $u = \theta$  (Fig. 2(a)), provided  $(S, \omega(0))$  is excitable [11].

- The moment at  $(Q, R)$  admits a one-to-one relation with the steady-state of output  $\varpi$  of the (swapped) interconnection between system (1) and the filter

$$\dot{\varpi} = Q\varpi + R\eta \quad (8)$$

via  $\eta = y$  (Fig. 2(b)), for  $x(0) = \varpi(0) = 0$  and any non-zero signal  $u$  that exponentially decays to zero. ■

Taking a step back, the mere satisfaction of (3) and (4) (without the additional assumptions in Theorem 1) implies the existence of two invariant subspaces, namely  $\overline{\mathcal{M}}_d =$

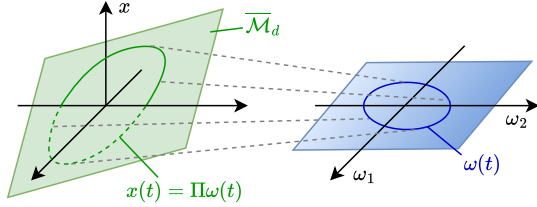


Fig. 3. Visualisation of the Subspace  $\bar{\mathcal{M}}_d$ .

$\{(x, \omega) \in \mathbb{R}^{n+\hat{n}} \mid x = \Pi\omega\}$  in Fig. 2(a) when  $u = \theta$ ; and  $\bar{\mathcal{M}}_s = \{(x, \varpi) \in \mathbb{R}^{n+\hat{n}} \mid \varpi = -\Upsilon x\}$  in Fig. 2(b) when  $u \equiv 0$ . Moreover, under the assumptions of Theorem 1, it is possible to show [12] that the dynamics on the globally exponentially attractive subspace  $\bar{\mathcal{M}}_d$ , visualised in Fig. 3, are described by

$$\dot{\omega} = S\omega, \quad \text{and} \quad y = C\Pi\omega. \quad (9)$$

Similarly, the dynamics of the error variable  $\zeta = \varpi + \Upsilon x$  are described by

$$\dot{\zeta} = Q\zeta + \Upsilon Bu. \quad (10)$$

Thus,  $C\Pi$  is the steady-state observation matrix relating  $y$  to the state  $\omega$  of the signal generator, while  $\Upsilon B$  influences how the control  $u$  impacts the deviation from the invariant subspace  $\bar{\mathcal{M}}_s$  [12]. Then one can see that the intuition behind the reduced-order model (5) is that when  $u$  is generated by (7) and  $A$  and  $S - GL$  are Hurwitz, then (1) and (5) have the same asymptotic behaviour, which is described by (9). A similar intuition holds for the swapped interconnection. These observations are important for reinterpreting the ASHC technique in the next section.

In the context of model reduction, the benefit brought by Theorem 1 lies in extending the notion of moment to general classes of systems, such as nonlinear and time-delay systems, see *e.g.* [13], and providing data-driven approaches through the use of the invariant manifolds  $\bar{\mathcal{M}}_d$  and  $\bar{\mathcal{M}}_s$  [14], [15].

### B. Approximate-Simulation-based Hierarchical Control

Now we turn our focus to the ASHC technique, recalling its two key requirements. The ASHC technique aims to design a simpler abstract system and an interface function  $u_v : \mathbb{R}^{\hat{m}} \times \mathbb{R}^{\hat{n}} \times \mathbb{R}^n \rightarrow \mathbb{R}^m$  to achieve the control synthesis of the large-scale system with lower computational costs, see Fig. 1. To provide guarantees on the trajectories of the large-scale system, the first key requirement is that the error between the output trajectories of the large-scale and simpler systems is bounded through a so-called ‘‘simulation function’’ [4], [16], defined as follows.

**Definition 2 ([4]):** Let  $V : \mathbb{R}^{\hat{n}} \times \mathbb{R}^n \rightarrow \mathbb{R}_{\geq 0}$  be a smooth function and  $u_v : \mathbb{R}^{\hat{m}} \times \mathbb{R}^{\hat{n}} \times \mathbb{R}^n \rightarrow \mathbb{R}^m$  be a continuous function.  $V$  is a *simulation function* of system (2) by system (1), and  $u_v$  is an associated *interface*, if there exists a class- $\mathcal{K}$  function  $\gamma$  such that for all  $(\xi, x) \in \mathbb{R}^{\hat{n}} \times \mathbb{R}^n$ ,  $V(\xi, x) \geq \|H\xi - Cx\|$ , and for all  $v \in \mathbb{R}^{\hat{m}}$  satisfying  $\gamma(\|v\|) < V(\xi, x)$ , then  $\frac{\partial V(\xi, x)}{\partial \xi}(F\xi + Gv) + \frac{\partial V(\xi, x)}{\partial x}(Ax + Bu_v(v, \xi, x)) < 0$ . ■

In fact, the above simulation and interface functions guarantee that the error between the output trajectories

$\psi$  and  $y$  of two systems satisfies  $\|\psi(t) - y(t)\| \leq \max\{V(\xi(0), x(0)), \gamma(\|v\|_{\infty})\}$  for all  $t \geq 0$ , see [4, Theorem 1] for more details.

Before looking at how to design the simulation function and the interface, the following standard assumption is introduced.

**Assumption 1:** System (1) is stabilisable.

Then we have the following results.

**Lemma 1 ([4]):** Suppose Assumption 1 holds. Then there exists a positive definite symmetric matrix  $W \in \mathbb{R}^{n \times n}$  and a strictly positive scalar  $\lambda$  such that

$$W \succeq C^T C, \quad (A + BK)^T W + W(A + BK) \preceq -2\lambda W,$$

with  $K \in \mathbb{R}^{m \times n}$  any matrix such that  $\sigma(A + BK) \subset \mathbb{C}_{<0}$ . ■

**Theorem 2 ([4]):** Suppose Assumption 1 holds and assume there exist matrices  $P \in \mathbb{R}^{n \times \hat{n}}$  and  $\hat{L} \in \mathbb{R}^{m \times \hat{n}}$  solving the linear matrix equations

$$PF = AP + B\hat{L}, \quad (11a)$$

$$H = CP. \quad (11b)$$

Then, the function  $V(\xi, x) := \sqrt{(P\xi - x)^T W (P\xi - x)}$  is a simulation function of system (2) by (1) and the associated interface takes the form

$$u_v(v, \xi, x) := \hat{R}v + \hat{L}\xi + K(x - P\xi), \quad (12)$$

for any matrix  $\hat{R} \in \mathbb{R}^{m \times \hat{m}}$ . ■

The second key requirement of the ASHC technique focuses on recovering any output trajectory generated by the large-scale system. This requirement is formulated as ‘‘for any output of the concrete system, we can construct an input of the abstraction such that this produces the same output’’. This is reminiscent, but different, of moment matching, which instead requires that the simpler model possess the same steady state when subject to the same input generated by (7). The ASHC requirement is specified as follows.

**Definition 3 ([4]):** System (2) is *M-related* to system (1) if there exists a matrix  $M \in \mathbb{R}^{\hat{n} \times n}$  such that for all  $x \in \mathbb{R}^n$  and  $u \in \mathbb{R}^m$ , there exists  $v \in \mathbb{R}^{\hat{m}}$  satisfying

$$M(Ax + Bu) = FMx + Gv, \quad (13a)$$

$$C = HM. \quad (13b)$$

Note that the *M*-relation yields that for any state trajectories of system (1) with any input function  $u$ , there exists an input function  $v$  to the simpler system (2) such that the subspace  $\mathcal{M}_s = \{(x, \xi) \mid \xi = Mx\}$  is invariant, see [7] for more details. Then the following result holds on the output level.

**Theorem 3 ([4]):** If system (2) is *M-related* to (1), then for any output trajectory  $y$  of system (1),  $\psi = y$  is an output trajectory of system (2) for some input function  $v$ . ■

To summarize, the ASHC technique for the large-scale system (1) is solved if one can design a simpler system (2) and an interface (12) that satisfies both (11), which guarantees the boundedness of the error between output trajectories of the two systems, and (13), which avoids the loss of controllable behaviours of system (1) when constructing the abstract system (2). These two requirements are viewed next through the lens of moment matching.

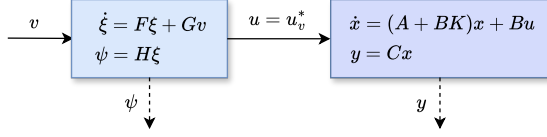


Fig. 4. Interconnection for the interpretation of the linear matrix equations (11) with a stabilising link  $u_v^* = \hat{R}v + (\hat{L} - KP)\xi$ .

### III. ASHC IN THE MOMENT MATCHING FRAMEWORK

In this section, we establish the connection between moment matching and ASHC techniques by reinterpreting the two key requirements posed by the ASHC technique explained in Section II through the lens of the direct and swapped interconnections in Fig. 2. To this end, we first look at the bounded output discrepancy requirement and study the  $M$ -relation requirement after that.

#### A. Bounded Output Discrepancy

The first design requirement of the ASHC technique is that the discrepancy between the output trajectories of the large-scale system (1) controlled by an interface (12), and the simpler system (2) is bounded by a simulation function. Recall that Theorem 2 yields that, under Assumption 1, the output discrepancy remains bounded for any input  $v \in L^\infty$  if there exist  $P \in \mathbb{R}^{n \times \hat{n}}$  and  $\hat{L} \in \mathbb{R}^{m \times \hat{n}}$  solving (11).

Since Theorem 1 points out the one-to-one relations between moments and steady-state responses, we reinterpret equations (11), together with the interface function (12), in the moment matching framework. To this end, for specific configurations, the hierarchical structure shown in Fig. 1 can be regarded as a cascade interconnection similar to the ones in Fig. 2. Hereto, denote the interface  $u_v$  in (12) as  $u_v = \hat{R}v + \hat{L}\xi + K(x - P\xi) = Kx + u_v^*$  with  $u_v^* = \hat{R}v + (\hat{L} - KP)\xi$ . Then the hierarchical structure in Fig. 1 is equivalent to the interconnection shown in Fig. 4, where system (2) is cascaded with the system

$$\dot{x} = (A + BK)x + Bu, \quad y = Cx, \quad (14)$$

via the link  $u = u_v^* = \hat{R}v + (\hat{L} - KP)\xi$ , with  $K$  such that  $\sigma(A + BK) \subset \mathbb{C}_{<0}$ . We first study the case for  $v \equiv 0$ , for which we have the following result.

**Theorem 4:** Consider the hierarchical structure shown in Fig. 1 and, equivalently, Fig. 4. Suppose  $v \equiv 0$  and Assumption 1 holds. Let  $F \in \mathbb{R}^{\hat{n} \times \hat{n}}$  be any matrix with simple eigenvalues satisfying  $\sigma(F) \subset \mathbb{C}_0$  and  $\sigma(F) \cap \sigma(A) = \emptyset$ . Let  $\hat{L}$  and  $K$  in (12) be such that  $(F, \hat{L})$  is observable and  $\sigma(A + BK) \subset \mathbb{C}_{<0}$ . Let  $P \in \mathbb{R}^{n \times \hat{n}}$  be the unique solution of (11a) and let the pair  $(F, \xi(0))$  be excitable. Then, there exists a one-to-one relation between the moment  $CP$  of system (1) at  $(F, \hat{L})$  and the steady-state output  $y$  of system (1) in Fig. 4.

*Proof:* Following Definition 1, as  $\sigma(F) \cap \sigma(A) = \emptyset$  and  $(F, \hat{L})$  is observable,  $CP$  is the moment of system (1) at  $(F, \hat{L})$ . When  $v \equiv 0$ , the hierarchical structure in Fig. 4, can be regarded as a direct interconnection formed by the generator (2) and system (14). Since  $\sigma(F) \cap \sigma(A + BK) = \emptyset$

and the pair  $(F, \hat{L} - KP)$  is observable (which we prove later),  $C\bar{P}$  denotes the moment of (14) at  $(F, \hat{L} - KP)$ , where  $\bar{P} \in \mathbb{R}^{n \times \hat{n}}$  is the unique solution to

$$\bar{P}F = (A + BK)\bar{P} + B(\hat{L} - KP), \quad (15)$$

with  $P$  solving (11a), see Definition 1. By subtracting (11a) from (15), we obtain  $(\bar{P} - P)F = A(\bar{P} - P) + B\hat{L} + BK(\bar{P} - P) - B\hat{L} = (A + BK)(\bar{P} - P)$ . Since  $\sigma(F) \cap \sigma(A + BK) = \emptyset$ , it follows that  $\bar{P} = P$ . Hence, the moment  $C\bar{P}$  of system (14) at  $(F, \hat{L} - KP)$  coincides with the moment  $CP$  of system (1) at  $(F, \hat{L})$ , and, by Theorem 1, has a one-to-one relation with the steady-state output  $y$  with  $v \equiv 0$  as the pair  $(F, \hat{L} - KP)$  is observable. To show this observability property, we assume, by contradiction, that the pair  $(F, \hat{L} - KP)$  is not observable, *i.e.*, by the PBH test, there exists a non-zero vector  $\varepsilon \in \mathbb{R}^{\hat{n}}$  such that  $F\varepsilon = \lambda_F\varepsilon$  and  $(\hat{L} - KP)\varepsilon = 0$  with  $\lambda_F \in \sigma(F)$ . Then right-multiplying  $\varepsilon$  to both sides of (15) implies  $(\lambda_F I_n - A - BK)\bar{P}\varepsilon = B(\hat{L} - KP)\varepsilon = 0$ . Since  $\sigma(F) \cap \sigma(A + BK) = \emptyset$ ,  $\text{rank}(\lambda_F I_n - A - BK) = n$  and therefore  $\bar{P}\varepsilon = P\varepsilon = 0$ . Consequently,  $(\hat{L} - KP)\varepsilon = \hat{L}\varepsilon = 0$ , which, by PBH test, contradicts the observability of  $(F, \hat{L})$ . Therefore, the pair  $(F, \hat{L} - KP)$  is observable, and this concludes the proof.  $\blacksquare$

The result of Theorem 4 provides a moment matching perspective of the bounded output discrepancy requirement. Following the proof of Theorem 4, system (2) with  $G = 0$  is the same as system (9), for  $S = F$  and  $L = \hat{L}$  (and so  $\Pi = P$ ). Thus, the abstract system with  $H = CP$  behaves as a “limiting” reduced-order model. It should be stressed that the abstract system is not of the form (5), because  $G = 0$ , and consequently it does not match the moments  $CP$  at  $(F, \hat{L})$ . But, as explained in Section II-A, the limiting system (9) is the system towards which the reduced-order model (5) tends to when  $u$  is driven by (7) via  $u = \theta$  and  $S - GL$  is Hurwitz. Thus, even though the abstract system is not a reduced-order model by moment matching, it still has the property of matching, for  $v \equiv 0$ , the steady-state output  $y$  of the large-scale system (1).

Continuing with this steady-state matching analysis, we now study the case when the input  $v \not\equiv 0$ . By denoting  $e_s = x - P\xi$ , the satisfaction of (11) and (12) implies

$$\begin{aligned} \dot{e}_s &= Ax + Bu_v - PF\xi - PGv \\ &= Ae_s + AP\xi + B\hat{R}v + B\hat{L}\xi + BK e_s - PF\xi - PGv \\ &= (A + BK)e_s + (B\hat{R} - PG)v, \end{aligned} \quad (16)$$

where  $K$  is such that  $\sigma(A + BK) \subset \mathbb{C}_{<0}$ . Now by (11b), the discrepancy in the output trajectories of two systems satisfies  $e_y = y - \psi = Cx - H\xi = Ce_s$ . On the one hand, this relation coincides with the previous statement that when  $v \equiv 0$ , the set  $\mathcal{M}_d = \{(x, \xi) | x = P\xi\}$  is exponentially attractive and invariant for all  $(x(0), \xi(0)) \in \mathbb{R}^{n+\hat{n}}$ . This results in the exponential decay of  $e_y$  to zero and the matching of the steady states of the two output trajectories  $\psi$  and  $y$ . On the other hand, when  $v \not\equiv 0$ , exponential stability of (16) implies that  $e_s$  (and  $e_y$ ) are bounded for any input  $v \in L^\infty$ . This result is consistent with the target of the ASHC technique. In summary, when  $v \equiv 0$ , the steady-state outputs are matched,

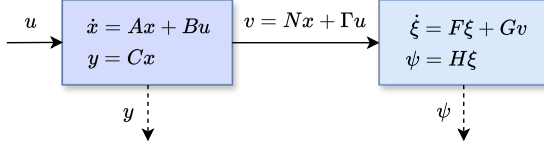


Fig. 5. Interconnection for the interpretation of the linear matrix equations (17).

and when  $v \neq 0$ , the two outputs have a bounded error, which can be minimized by an opportune selection of  $\hat{R}$  in (12).

*Remark 2:* The matching of the steady-state outputs of the two systems (1) and (2) when  $v \equiv 0$  is consistent with Definition 2, because the simulation function guarantees that  $\|\psi(t) - y(t)\|$  decays to zero as  $\gamma(\|v(t)\|) = 0$  for all times.

### B. $M$ -relation

Now we discuss the second key design requirement in the ASHC technique: the  $M$ -relation. To this end, we first show that the  $M$ -relation requirement (13) can also be characterised by Sylvester equations.

*Theorem 5:* System (2) is  $M$ -related to system (1) if there exist matrices  $N \in \mathbb{R}^{\hat{m} \times n}$  and  $\Gamma \in \mathbb{R}^{\hat{m} \times m}$  solving

$$MA = FM + GN, \quad (17a)$$

$$GT = MB, \quad (17b)$$

$$C = HM, \quad (17c)$$

for some matrix  $M \in \mathbb{R}^{\hat{n} \times n}$ .

*Proof:* Consider the right side of (13a). By substituting  $v = Nx + \Gamma u$ , we have  $FMx + Gv = FMx + GNx + G\Gamma u = MAx + MBu = M(Ax + Bu)$ , where we have used (17a) and (17b). From here, we conclude that (17) implies (13), proving the claim. ■

Theorem 5 proposes a sufficient condition for the  $M$ -relation based on a Sylvester equation and the restriction that the input  $v$  that drives system (2) takes the form

$$v = Nx + \Gamma u. \quad (18)$$

This restriction, in fact, is naturally satisfied by the existing geometric method proposed by [4] for finding a valid simpler system that satisfies both (11) and (13). The method is summarised as follows.

*Theorem 6 ([4]):* Consider the systems (1) and (2). Let

- $P \in \mathbb{R}^{n \times \hat{n}}$  be an injective map such that  $\text{im}(AP) \subseteq \text{im}(P) + \text{im}(B)$  and  $\text{im}(P) + \ker(C) = \mathbb{R}^n$ ;
- $D \in \mathbb{R}^{n \times (\hat{m}-m)}$ ,  $E \in \mathbb{R}^{(\hat{m}-m) \times n}$ , and  $M \in \mathbb{R}^{\hat{n} \times n}$  satisfy  $\text{im}(D) \subseteq \ker(C)$ ,  $\text{im}(P) \oplus \text{im}(D) = \mathbb{R}^n$ ,  $MP = I_{\hat{n}}$ , and  $PM + DE = I_n$ ;
- $F \in \mathbb{R}^{\hat{n} \times \hat{n}}$  and  $\hat{L} \in \mathbb{R}^{m \times \hat{n}}$  be such that  $AP = PF - B\hat{L}$ ;
- $H = CP$  and  $G = [MB \quad MAD]$ .

Then, (11) and (13) hold and therefore system (2) is  $M$ -related to (1). ■

By straightforward computations, this geometric design method proposed in Theorem 6 also satisfies (17) with

$$N = \begin{bmatrix} -\hat{L}M \\ E \end{bmatrix}, \quad \Gamma = \begin{bmatrix} I_m \\ 0_{(\hat{m}-m) \times m} \end{bmatrix}. \quad (19)$$

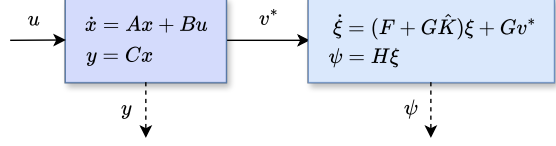


Fig. 6. Interconnection for the interpretation of the linear matrix equations (17) with a stabilising link  $v^* = \Gamma u + (N - K M)x$ .

Note that this inherently implies that the dimension  $\hat{m}$  of the input  $v$  to the simpler system (2) is larger than the dimension  $m$  of the input  $u$  to the large-scale system (1), *i.e.*,  $\hat{m} > m$ . This is natural in the ASHC technique but not expected in MOR techniques.

Through Theorem 5, the  $M$ -relation requirement can also be interpreted from the perspective of moment matching. In particular, this interpretation is based on the interconnection structure formed by system (2) and system (1) via the link (18), which is depicted in Fig. 5. Then we have the following result.

*Theorem 7:* Consider the interconnection shown in Fig. 5. Suppose  $u \equiv 0$  and  $A$  has simple eigenvalues satisfying  $\sigma(A) \subset \mathbb{C}_0$ . Suppose  $F$  is Hurwitz. Let  $N \in \mathbb{R}^{\hat{m} \times n}$  be such that  $(A, N)$  is observable. Let  $M \in \mathbb{R}^{\hat{n} \times n}$  be such that (17a) holds and let the pair  $(A, x(0))$  be excitable. Then, there exists a one-to-one relation between the moment  $HM$  of system (2) at  $(A, N)$  and the steady-state output  $\psi$ .

*Proof:* The result follows directly from Theorem 1. ■

As the  $M$ -relation requirement induces the invariant set  $\mathcal{M}_s = \{(x, \xi) \mid \xi = Mx\}$ , we can study, similarly to (16), the dynamics of the error  $\varepsilon_s = \xi - Mx$ . The satisfaction of (17) yields that  $\dot{\varepsilon}_s = F\xi + Gv - MAx - MBu = F\xi + GNx + GTu - (FM + GN)x - MBu = F\varepsilon_s$ , and the error in the output of two systems satisfies  $\varepsilon_y = \psi - y = H\xi - Cx = H\varepsilon_s$ . This result demonstrates that, starting with any initial condition  $(x(0), \xi(0)) \in \mathcal{M}_s$ , the  $M$ -relation yields the exact matching of the two output trajectories  $y$  and  $\psi$  in the direct interconnection shown in Fig. 5 for any input  $u$ . Conversely, if  $(x(0), \xi(0)) \notin \mathcal{M}_s$ , these output trajectories will match at the steady state only if  $F$  is Hurwitz, *i.e.*, only if the invariant set  $\mathcal{M}_s$  is also attractive, as assumed by Theorem 7.

If  $F$  is not Hurwitz (as  $\sigma(F)$  may be used to define the desired moments in Theorem 4), the input  $v$  in (18) can also be modified to render  $\mathcal{M}_s$  both invariant and attractive for the same  $M$ . Assume the pair  $(F, G)$  is stabilisable, *i.e.*, there exists a matrix  $\hat{K} \in \mathbb{R}^{\hat{m} \times \hat{n}}$  such that  $\sigma(F + G\hat{K}) \subset \mathbb{C}_{<0}$ . Then the input

$$v = Nx + \Gamma u + \hat{K}(\xi - Mx) \quad (20)$$

leads to  $\dot{\varepsilon}_s = (F + G\hat{K})\varepsilon_s$ . Therefore, the invariant set  $\mathcal{M}_s$  is exponentially attractive. This result shows that the  $M$ -relation alternatively means that for any state  $x$  with any inputs  $u$  into system (1), there exists an input  $v$  to system (2) such that the steady-state outputs of two systems,  $\psi$  and  $y$ , are the same for all initial conditions  $x(0)$  and  $\xi(0)$ . Consequently, a similar matching result as Theorem 4 exists, which relaxes the stability assumption on system (2) of Theorem 7.

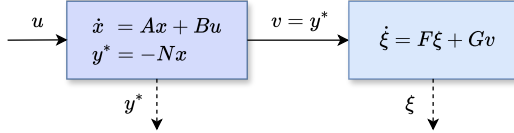


Fig. 7. Swapped interconnection for the interpretation of the linear matrix equations (17).

*Corollary 1:* Consider the interconnection structure shown in Fig. 6. Suppose  $u \equiv 0$ , the pair  $(F, G)$  is stabilisable, and  $A$  has simple eigenvalues satisfying  $\sigma(A) \subset \mathbb{C}_0$  and  $\sigma(A) \cap \sigma(F) = \emptyset$ . Let  $N \in \mathbb{R}^{\hat{m} \times n}$  and  $\hat{K} \in \mathbb{R}^{\hat{m} \times \hat{n}}$  in (20) be such that  $(A, N)$  is observable and  $\sigma(F + G\hat{K}) \subset \mathbb{C}_{<0}$ . Let  $M \in \mathbb{R}^{\hat{n} \times n}$  be such that (17a) holds and let the pair  $(A, x(0))$  be excitable. Then, there exists a one-to-one relation between the moment  $HM$  of system (2) at  $(A, N)$  and the steady-state output  $\psi$  of system (2) in the interconnection in Fig. 6.

*Proof:* The proof is similar to that of Theorem 4 and, thus, is omitted. ■

*Remark 3:* By the previous derivations of the error dynamics  $\varepsilon_s$  and  $\varepsilon_y$ , the assumption that the eigenvalues of  $A$  are simple and satisfy  $\sigma(A) \subset \mathbb{C}_0$  in Theorem 7 and Corollary 1 is only used for guaranteeing the existence of non-trivial steady-state responses of the outputs  $y$  and  $\psi$ . This assumption is not necessary for  $\varepsilon_s$  and  $\varepsilon_y$  to converge to zero.

Now we provide an alternative interpretation. Rather than interpreting the  $M$ -relation requirement (17) using the direct interconnections in Figs. 5 and 6, it is possible to interpret this requirement as a type of swapped interconnection introduced in Section II-A as shown in the next result.

*Theorem 8:* Consider the interconnection shown in Fig. 7. Suppose  $\sigma(A) \subset \mathbb{C}_{<0}$ . Let  $F$  have simple eigenvalues satisfying  $\sigma(F) \subset \mathbb{C}_0$  and  $\sigma(F) \cap \sigma(A) = \emptyset$ . Assume the pair  $(F, G)$  is reachable. Let  $M \in \mathbb{R}^{\hat{n} \times n}$  be such that (17a) holds. Then, there exists a one-to-one relation between the moment  $MB$  of system

$$\dot{x} = Ax + Bu, \quad y^* = -Nx, \quad (21)$$

at  $(F, G)$ , with  $y^*(t) \in \mathbb{R}^{\hat{m}}$ , and the steady-state response of output  $\xi$  with  $x(0) = \xi(0) = 0$  for any non-zero signal  $u$  that exponentially decays to zero.

*Proof:* The result follows directly from Theorem 1. ■

Note that the matrix  $MB$  is not the moment of system (1), but that of system (21), which flows as (1), but has a different output  $y^* = -Nx$ , where  $-N$  is not necessarily equal to  $C$ . Moreover, Theorem 6 implies that a simpler system that satisfies the  $M$ -relation (17) can be designed with  $G = [MB \quad MAD]$  and with  $N$  and  $\Gamma$  in (19). Thus, system (2) with  $H = 0$  is the same as system (10), for  $Q = F$ ,  $R = G$ ,  $C = -N$  (and so  $\Upsilon = M$ ) and  $v = \Gamma u$ . The resulting abstract system takes the form

$$\dot{\xi} = F\xi + MBu.$$

Thus, in a dual fashion with respect to the discussion after Theorem 4, the abstract system with input  $v = \Gamma u$  behaves as

a “*limiting*” reduced-order model. It should be stressed that the abstract system is not of the form (6), because  $H = 0$ , and consequently it does not match the moments  $MB$  at  $(F, G)$ . But, as explained in Section II-A, the limiting system (10) is the system towards which the reduced-order model (6) tends to when  $Q - RH$  is Hurwitz. Thus, even though the abstract system is not a reduced-order model by moment matching, it still has the property of matching, for any non-zero signal  $u$  that exponentially decays to zero, the steady-state output of the swapped interconnection in Fig. 7.

### C. Brief Summary of the Two Key Requirements

We briefly summarise the interpretations presented above. The ASHC technique consists of designing a simpler system and an interface such that: i) the output responses of the two systems have bounded discrepancy; ii) the simpler system is  $M$ -related to the large-scale system. Regarding requirement i), we have the following interpretations.

- When the input  $v \equiv 0$ , we provide conditions under which the steady-state output of system (1) in the direct interconnection shown in Fig. 4 is matched with the steady-state output of system (2). In other words, the steady-state output response of system (1) admits a one-to-one relation with the moments of system (1) at  $(F, \hat{L})$ , see Theorem 4.
- When the input  $v \neq 0$  but  $v \in L^\infty$ , the mismatch between the steady-state outputs of the two systems, interconnected via the interface, is bounded and can be minimized.

Regarding requirement ii), we have the following interpretations.

- For any bounded input  $u$ , we provide conditions under which the steady-state output of system (2) in the direct interconnections shown in Fig. 5 and Fig. 6 is matched with the steady-state response of system (1). In other words, the steady-state output response of system (2) admits a one-to-one relation with the moments of system (2) at  $(A, N)$ , see Theorem 7 and Corollary 1.
- When the input  $u$  is any non-zero signal that exponentially decays to zero, we provide conditions under which the steady-state output of the swapped interconnection shown in Fig. 7 admits a one-to-one relation with the moments of system (21) at  $(F, G)$ , see Theorem 8.

In summary, the final obtained abstract system, for  $v = \Gamma u$ , namely

$$\dot{\xi} = F\xi + MBu, \quad \psi = CP\xi, \quad (22)$$

is reminiscent of the two-sided reduced-order model by moment matching, in the “*limiting*” sense described in the previous sections.

### D. Discussion

The importance of this paper lies in bridging the conceptual gap between moment matching and the ASHC technique. The moment matching method has an advantage of admitting natural extensions beyond LTI systems, such as nonlinear systems [17], time-delay systems [13], and stochastic

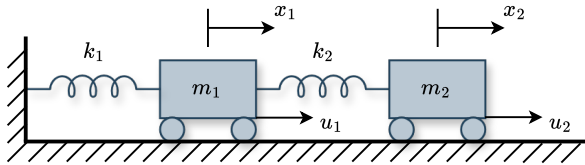


Fig. 8. Two-spring two-mass mechanical system.

systems [18]. Meanwhile, other techniques, such as data-driven methods, have also been proposed for solving moment matching problems [14], [15]. Those directions have been partly, but not extensively, explored in the ASHC context. Bridging the gap between these two techniques suggests that the existing results in the moment matching field can potentially lead to extensions of the ASHC method to more generic settings. Conversely, the current developments in the ASHC technique, *e.g.*, compositional method for constructing abstractions for networked systems [19], [20] and symbolic control method for implementing approximate simulations [21], do not have a counterpart in the moment matching framework.

To give a concrete hint of this potential, we consider the development of a nonlinear ASHC framework. Since we have characterised the objects that define the final abstraction (22) by means of the Sylvester equations (11) and (17), by leveraging the nonlinear moment matching framework, a nonlinear abstraction can be characterised by means of the invariance equations [3, (28) and (35)] *mutatis mutandis*. A work in this direction is already in preparation.

#### IV. NUMERICAL EXAMPLE

We illustrate the theory presented in the paper by means of a practical example. We study the ASHC problem of system (1) with matrices

$$A = \begin{bmatrix} 0 & 0 & 1 & 0 \\ 0 & 0 & 0 & 1 \\ -\frac{k_1+k_2}{m_1} & \frac{k_2}{m_1} & 0 & 0 \\ \frac{k_2}{m_2} & -\frac{k_2}{m_2} & 0 & 0 \end{bmatrix}, \quad B = \begin{bmatrix} 0 & 0 \\ 0 & 0 \\ \frac{1}{m_1} & 0 \\ 0 & \frac{1}{m_2} \end{bmatrix},$$

and  $C = [I_2, 0_{2 \times 2}]$ , where the system dimensions  $n = 4$ ,  $m = p = 2$ . This concrete system models the two-spring two-mass mechanical system in Fig. 8, which consists of two masses  $m_1$  and  $m_2$  connected by two springs with spring coefficients  $k_1$  and  $k_2$ . Variables  $x_1$  and  $x_2$  denote the displacements from the equilibrium positions of the masses  $m_1$  and  $m_2$  under the control forces  $u_1$  and  $u_2$ , respectively. Then the input, output, and state variables of system (1) are denoted as  $u = [u_1, u_2]^\top$ ,  $y = [x_1, x_2]^\top$ , and  $x = [x_1, x_2, x_3, x_4]^\top$  with  $x_3 = \dot{x}_1$  and  $x_4 = \dot{x}_2$ . In the following simulation, we select the parameters as  $k_1 = 100$  N/m,  $k_2 = 50$  N/m,  $m_1 = 20$  kg, and  $m_2 = 10$  kg. Then by following the design method proposed by Theorem 6, a valid simpler model (2) solving the ASHC problem is given by the selection

$$F = \begin{bmatrix} 0 & 10 \\ -10 & 0 \end{bmatrix}, \quad G = \begin{bmatrix} 0 & 0 & 1 & 0 \\ 0 & 0 & 0 & 1 \end{bmatrix}, \quad H = \begin{bmatrix} 1 & 0 \\ 0 & 1 \end{bmatrix},$$

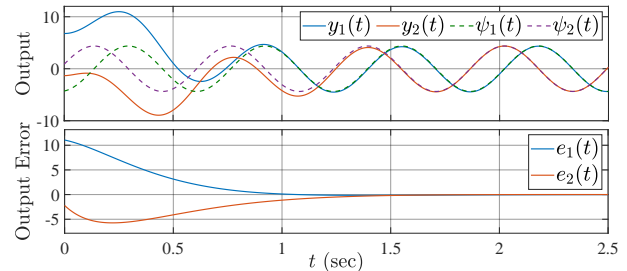


Fig. 9. Time histories of outputs  $y = [y_1, y_2]^\top$  (solid) and  $\psi = [\psi_1, \psi_2]^\top$  (dashed) of systems (1) and (2) in the interconnection in Fig. 4 (top) and their error  $e_y = [e_1, e_2]^\top = y - \psi$  (bottom) with  $v \equiv 0$ .

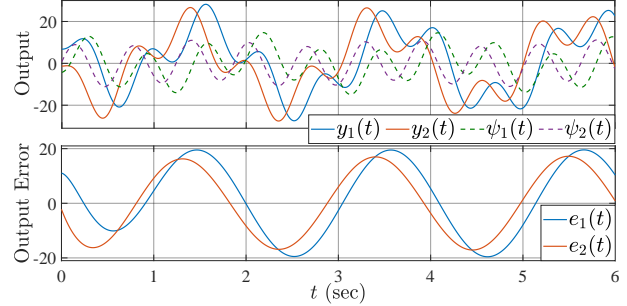


Fig. 10. Time histories of outputs  $y = [y_1, y_2]^\top$  (solid) and  $\psi = [\psi_1, \psi_2]^\top$  (dashed) of systems (1) and (2) in the interconnection in Fig. 4 (top) and their error  $e_y = [e_1, e_2]^\top = y - \psi$  (bottom) with  $v \not\equiv 0$ .

with dimensions  $\hat{n} = 2$  and  $\hat{m} = 4$ . In addition, the matrices

$$P = \begin{bmatrix} 1 & 0 & 0 & -10 \\ 0 & 1 & 10 & 0 \end{bmatrix}^\top, \quad \hat{L} = \begin{bmatrix} -1850 & -50 \\ -50 & -950 \end{bmatrix},$$

$M = [I_2, 0_{2 \times 2}]$ , and  $D = [0_{2 \times 2}, I_2]^\top$  solve (11) and satisfy the design requirements in Theorem 6. The matrix  $\hat{R}$  is selected with all entries equal to one. Furthermore, the matrices  $N$  and  $\Gamma$  are given by

$$N = \begin{bmatrix} -1850 & 50 & 0 & 0 \\ 50 & 950 & 0 & 0 \\ 0 & -10 & 1 & 0 \\ 10 & 0 & 0 & 1 \end{bmatrix}, \quad \Gamma = \begin{bmatrix} 1 & 0 \\ 0 & 1 \\ 0 & 0 \\ 0 & 0 \end{bmatrix},$$

solving (17) with  $M$  as above. Note that the matrices  $A$  and  $F$  both have simple eigenvalues located on the imaginary axis, namely  $\sigma(A) = \{\pm 3.1623i, \pm 1.5811i\}$  and  $\sigma(F) = \{\pm 10i\}$ . In addition, it can be verified that the pairs  $(A, B)$  and  $(F, G)$  are stabilisable. In what follows, we illustrate our interpretation of the ASHC technique in Section III by implementing the two interconnection frameworks shown in Figs. 4 and 6. The initial conditions of the two systems are randomly selected as  $x_0 = [6.7794, -1.3348, -0.5875, 1.2143]^\top$  and  $\xi_0 = [-4.2811, 0.8733]^\top$ .

We first implement the interconnection shown in Fig. 4, which is equivalent to the hierarchical structure used in the ASHC technique, and is used for interpreting the bounded output discrepancy requirement. The stabilising gain  $K$  is selected such that  $\sigma(A + BK) = \{-3 \pm 1.5i, -5 \pm 2i\}$ . Then we conduct simulations with  $v \equiv 0$  and  $v \not\equiv 0$  separately, where, when  $v \not\equiv 0$ , we arbitrarily choose  $v =$

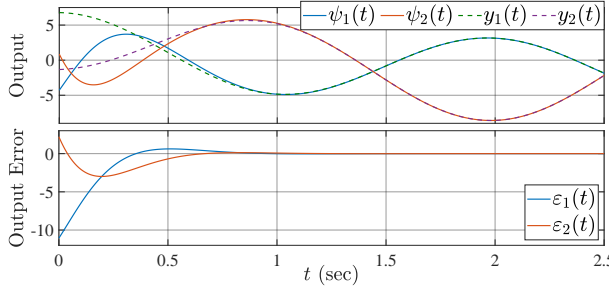


Fig. 11. Time histories of outputs  $y = [y_1, y_2]^\top$  (dashed) and  $\psi = [\psi_1, \psi_2]^\top$  (solid) of systems (1) and (2) in the interconnection in Fig. 6 (top) and their error  $\varepsilon_y = [\varepsilon_1, \varepsilon_2]^\top = \psi - y$  (bottom) with  $u \equiv 0$ .

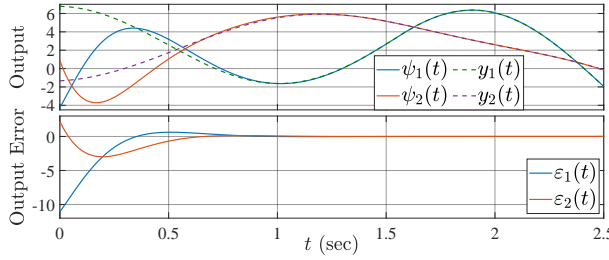


Fig. 12. Time histories of outputs  $y = [y_1, y_2]^\top$  (dashed) and  $\psi = [\psi_1, \psi_2]^\top$  (solid) of systems (1) and (2) in the interconnection in Fig. 6 (top) and their error  $\varepsilon_y = [\varepsilon_1, \varepsilon_2]^\top = \psi - y$  (bottom) with  $u \not\equiv 0$ .

$[51.032 \sin(4t), -25.945 \text{sign}(\sin(6t)), 0, 48.056 \cos(3t)]^\top$ . The results are shown in Figs. 9 and 10. Fig. 9 displays for  $v \equiv 0$  the time histories (top) of outputs  $y$  and  $\psi$  of the interconnection in Fig. 4 and (bottom) of their error  $e_y = y - \psi$ . The plots indicate that when  $v \equiv 0$ , the steady-state outputs of (the stabilised) system (1) in the interconnection in Fig. 4 and system (2) coincide with each other, suggesting that the moment matching result presented by Theorem 4 holds. The outputs and the corresponding error when  $v \not\equiv 0$  are shown in Fig. 10. In this case, the error between these two output trajectories is bounded, as anticipated by the results in Section III-A.

We finally implement the interconnection in Fig. 6 that is used for interpreting the  $M$ -relation requirement, which states that for any  $u$ , there exists an input  $v$  such that the output trajectories match. Again, we simulate the interconnection with  $u \equiv 0$  and  $u \not\equiv 0$  (arbitrarily set as  $u = [296.881 \text{sign}(\sin(2t)), -161.659 \cos(3t)]^\top$ ) separately, with the stabilising gain  $\hat{K}$  selected such that  $\sigma(F + G\hat{K}) = \{-5 \pm 5i\}$ . The results of the simulations are depicted in Figs. 11 and 12, which show the time histories of (top) outputs  $\psi$  and  $y$  from the interconnection in Fig. 6 as well as (bottom) their difference  $\varepsilon_y = \psi - y$  when  $u \equiv 0$  (Fig. 11) and  $u \not\equiv 0$  (Fig. 12). The figures imply that when system (2) is  $M$ -related to system (1) with requirement (17) satisfied by a stabilisable pair  $(F, G)$ , then  $v$  as in (20) results in the matching of the steady-state outputs of the two (stabilised) systems in the interconnection in Fig. 6, no matter whether  $u \equiv 0$  or not. This result coincides with the discussions in Section III-B.

## V. CONCLUSION

In this paper, we have established a connection between moment matching and the ASHC techniques. We have also identified research directions that enable the use of moment-matching-based techniques in ASHC problems and the use of ASHC techniques in moment matching problems. These results are currently under development.

## REFERENCES

- [1] A. C. Antoulas, *Approximation of large-scale dynamical systems*. Philadelphia, USA: SIAM, 2005.
- [2] W. H. Schilders, H. A. Van der Vorst, and J. Rommes, *Model order reduction: theory, research aspects and applications*. Berlin, Heidelberg: Springer, 2008, vol. 13.
- [3] G. Scarciootti and A. Astolfi, “Interconnection-based model order reduction-a survey,” *Eur. J. Control*, vol. 75, p. 100929, 2024.
- [4] A. Girard and G. J. Pappas, “Hierarchical control system design using approximate simulation,” *Automatica*, vol. 45, no. 2, pp. 566–571, 2009.
- [5] M. Zamani and M. Arcak, “Compositional abstraction for networks of control systems: A dissipativity approach,” *IEEE Trans. Control Netw. Syst.*, vol. 5, no. 3, pp. 1003–1015, 2017.
- [6] A. Astolfi, “Model reduction by moment matching for linear and nonlinear systems,” *IEEE Trans. Autom. Control*, vol. 55, no. 10, pp. 2321–2336, 2010.
- [7] G. J. Pappas, G. Lafferriere, and S. Sastry, “Hierarchically consistent control systems,” *IEEE Trans. Autom. Control*, vol. 45, no. 6, pp. 1144–1160, 2000.
- [8] K. Gallivan, A. Vandendorpe, and P. Van Dooren, “Model reduction and the solution of Sylvester equations,” *MTNS, Kyoto, Japan*, vol. 50, 2006.
- [9] M. F. Shakib, G. Scarciootti, A. Y. Pogromsky, A. Pavlov, and N. van de Wouw, “Time-domain moment matching for multiple-input multiple-output linear time-invariant models,” *Automatica*, vol. 152, p. 110935, 2023.
- [10] A. Isidori, *Nonlinear control systems: an introduction*. Berlin, Heidelberg: Springer-Verlag, 1985.
- [11] A. Padoan, G. Scarciootti, and A. Astolfi, “A geometric characterization of the persistence of excitation condition for the solutions of autonomous systems,” *IEEE Trans. Autom. Control*, vol. 62, no. 11, pp. 5666–5677, 2017.
- [12] J. W. Simpson-Porco, D. Astolfi, and G. Scarciootti, “Steady-state cascade operators and their role in linear control, estimation, and model reduction problems,” *IEEE Trans. Autom. Control (to appear)*, 2026.
- [13] G. Scarciootti and A. Astolfi, “Model reduction of neutral linear and nonlinear time-invariant time-delay systems with discrete and distributed delays,” *IEEE Trans. Autom. Control*, vol. 61, no. 6, pp. 1438–1451, 2015.
- [14] —, “Data-driven model reduction by moment matching for linear and nonlinear systems,” *Automatica*, vol. 79, pp. 340–351, 2017.
- [15] J. Mao and G. Scarciootti, “Data-driven model reduction by two-sided moment matching,” *Automatica*, vol. 166, p. 111702, 2024.
- [16] A. Girard and G. J. Pappas, “Approximation metrics for discrete and continuous systems,” *IEEE Trans. Autom. Control*, vol. 52, no. 5, pp. 782–798, 2007.
- [17] F. Shakib, G. Scarciootti, M. Jungers, A. Y. Pogromsky, A. Pavlov, and N. van de Wouw, “Optimal model reduction by time-domain moment matching for Lur'e-type models,” *IEEE Trans. Autom. Control*, vol. 69, no. 12, pp. 8820–8827, 2024.
- [18] G. Scarciootti and A. R. Teel, “On moment matching for stochastic systems,” *IEEE Trans. Autom. Control*, vol. 67, no. 2, pp. 541–556, 2021.
- [19] M. Rungger and M. Zamani, “Compositional construction of approximate abstractions of interconnected control systems,” *IEEE Trans. Control Netw. Syst.*, vol. 5, no. 1, pp. 116–127, 2016.
- [20] S. W. Smith, M. Arcak, and M. Zamani, “Approximate abstractions of control systems with an application to aggregation,” *Automatica*, vol. 119, p. 109065, 2020.
- [21] P. Tabuada, “An approximate simulation approach to symbolic control,” *IEEE Transactions on Automatic Control*, vol. 53, no. 6, pp. 1406–1418, 2008.